

Si, Shuhao; Weigel, Christoph; Messerschmidt, Martin; Thesen, Manuel W.;  
Sinzinger, Stefan; Strehle, Steffen:

**A study of imprint and etching behavior on fused silica of a new tailored resist  
mr-NIL213FC for soft UV-NIL**

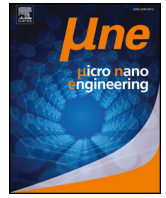
---

*Original published in:* Micro and nano engineering. - Amsterdam : Elsevier. - 6 (2020), art.  
100047, 7 pp.  
*Original published:* 2020-02-21  
*ISSN:* 2590-0072  
*DOI:* [10.1016/j.mne.2020.100047](https://doi.org/10.1016/j.mne.2020.100047)  
*[Visited:* 2020-05-18]



This work is licensed under a [Creative Commons Attribution 4.0 International](https://creativecommons.org/licenses/by/4.0/) license. To view a copy of this license, visit <https://creativecommons.org/licenses/by/4.0/>

---



## Research paper

## A study of imprint and etching behavior on fused silica of a new tailored resist mr-NIL213FC for soft UV-NIL

Shuhao Si<sup>a,\*</sup>, C. Weigel<sup>a</sup>, M. Messerschmidt<sup>b</sup>, M.W. Thesen<sup>b</sup>, S. Sinzinger<sup>a</sup>, S. Strehle<sup>a</sup><sup>a</sup> Technische Universität Ilmenau, IMN MacroNano®, Germany<sup>b</sup> Micro Resist Technology GmbH, Germany

## ARTICLE INFO

## Keywords:

Soft UV NIL  
Nanofabrication  
PDMS stamp  
Glass etching  
High etching selectivity  
New resist

## ABSTRACT

A new type of a specifically tailored resist for Soft Nanoimprint Lithography (Soft UV-NIL) namely mr-NIL213FC has been developed. It aims for a significant improvement of its etch-resistance with regard to underlying oxide substrates such as glass. This work demonstrates the first study of its imprint performance and etching behavior against fused silica wafers. First of all, the resist shows full compatibility with automated Soft UV-NIL using PDMS-based soft stamps and at ambient (oxygen containing) conditions for both step-and-repeat and full-wafer approaches. Moreover, the selectivity of the resist to the underlying fused silica substrate, in a high power and high etch rate condition, has reached to over 0.6, which is a significant step-up among most products in this context. The improved resistance of the resist facilitates direct etching processes for high resolution and high structure fidelity.

## 1. Motivation and overview

Nanostructures have been playing an essential role in the past decades ranging from single elements to system miniaturizations. Given the tremendous benefits, nanostructures such as nanopillars/holes, nanogratings/rods/wires, nanoparticles, and nanomesh/sheet/films emerged as capable components within the fields of photonics, MEMS/MOEMS/NEMS, biocompatible materials, energy harvesting, optics, pharmaceuticals, security features and so on [1–5]. In IC industry, the availability of advanced nanostructure assembly techniques powered the fulfillment of Moore's Law as well as the concept of "Beyond Moore's Law" [6–8]. Within the entire nanofabrication chain, lithography defines and realizes the required nanopatterns for application-oriented purposes. As one of the powerful and promising techniques of nanolithography, Nanoimprint Lithography (NIL) has been increasingly brought in use for both scientific and industrial fields due to the increasing demand of large area patterning, high throughput and most importantly low cost nanopatterning.

NIL using UV-curable material and soft molds (Soft UV-NIL) combine in principle UV-lithography and soft lithography. Especially when large area patterning and high throughput at low costs matters, the advantages of Soft UV-NIL enables to outperform other direct writing techniques.

Micro- and nano-photonics system is one of the perspective

application fields that Soft UV-NIL is engaged to a high extent. Various application fields, such as patterned sapphire substrates (PSS), photonic structures, surface texturing, photonic crystals, microdisks and surface plasmons can be realized reproducibly and at large scale based on the NIL technique. An individual application requires its corresponding substrate material. A variety of III-V semiconductor materials is for instance suitable to yield optoelectronic products such as nanoscale light sources, LEDs, and photonic crystals. Metals and metal-oxides have been applied for advanced nanoplasmonic sensing. In addition to silicon, silicon dioxide has also been widely engaged in applications that manipulate light such as polarizers for Liquid Crystal Displays (LCD), diffractive optical elements (DOE), wafer level optics (WLO), and waveguiding [9]. The significant increase in interest of nanopattern transfer processes for exotic substrate materials strongly motivates the investigation and development of new materials and processes.

Soft UV-NIL has been acknowledged as a powerful technique to boost large-scale and high-resolution nanostructure assemblies with high throughput and at low cost for the abovementioned applications. Despite that most hardware manufacturers offer their own process setups, materials and imprint schemes as a package, diverse perspectives affect the performance in general. One of the key issues are the inherent properties of NIL resist. On one hand, the resist should possess suitable coating properties with respect to the underlying substrate and a high compatibility to the contacting soft mold. On the other hand, the

\* Corresponding author.

E-mail address: [shuhao.si@tu-ilmenau.de](mailto:shuhao.si@tu-ilmenau.de) (S. Si).

resist is expected to possess a high resistance to the exposure of plasma during the pattern transfer, which will lead to a high selectivity to the material removal of the underlying substrate.

Under these circumstances, a variety of resist materials has been invented to fit into diverse and complex imprint setups and schemes. One of the simplest and most universal imprint conditions is to conduct the imprint in ambient atmosphere using a highly flexible Polydimethylsiloxane (PDMS)-based soft mold [10]. This can even be realized without an automated machine, given that the advantageous physical and chemical properties of PDMS. However, specific challenges of PDMS-based soft molds at ambient conditions exist when a non-tailored generic resist chemistry is used. For instance, although the air-permeability is always considered as an advantage that allows trapped air in the structure cavity to diffuse out, the oxygen from the outside of the soft mold can as well diffuse continuously into the resist. This inward diffused oxygen may inhibit the curing of the generic resist [11]. In addition, the complex components of the resist can also diffuse into the PDMS, i.e. smaller molecules of resist can fill up the relatively large space due to the relatively low polymer network density of PDMS. Hence, this increases the risk that the resist can stick to the surface of soft mold, which causes non-removable contamination. In severe cases, the diffusion may result in a complete rip-off of the coated resist.

There have been diverse tailored resists existing on the market to address these issues and overcome these challenges when PDMS-based soft molds are in use at ambient atmosphere, such as the well acknowledged mr-NIL210 series [12]. Based on the outstanding performance of the mr-NIL210 series, a new fast curing (FC) technology has been introduced recently to overcome the oxygen inhibition effect which can occur during soft UV-NIL with PDMS based soft working stamps [13]. In this work we will present the specifically tailored resist formulation namely mr-NIL213FC (fast cure). The imprint properties from the previous mr-NIL210 series are has been maintained, and meanwhile to step further, the new resist is aiming for a significant improvement of its etch-resistance while being exposed to plasma to increase the etch selectivity with regard to the underlying substrate. With respect to complex substrates for micro- and nanostructure patterning like glass, it is common to bring in an additional layer as hard etch-mask, e.g. nickel, to etch for a sufficient depth [14]. However, in nanostructure patterning and for special materials and applications, it is not allowed to go through an extra process for metallic material. Also, the removal of metal in nanostructure patterning challenge the overall process chain. Therefore, there is a significant need for advanced resists that provide sufficient resistance to plasma etching enabling the use of a less redundant material.

In this work, a first demonstration of nanoimprint using the new resist mr-NIL213FC, with PDMS-based soft mold, on full wafer scale, at ambient atmosphere is shown. To begin with, fused silica ( $\text{SiO}_2$ ), one of the most widely used materials for optical and photonic applications, is employed. A step further, a first study and experimental investigation of etching behavior of the new resist with respect to underlying fused silica substrates in  $\text{CHF}_3$  and/or  $\text{CF}_4$  chemistry is carried out.

## 2. The soft UV-NIL setup

A full process chain of NIL is performed for the demonstration and investigation. To start with, a 100 mm silicon nanopillar master featuring a diameter of 400 nm, pitch of 1000 nm and depth of approx. 840 nm is prepared (Fig. 1a). This master is replicated and the feature size is shrunken from a commercial master with a diameter of 600 nm, by using a method named *NanoTuFe* approach [10] and etched on our side.

After thorough cleaning of the silicon master, an anti-sticking layer (ASL) using material 1H, 1H, 2H, 2H-Perfluorodecyltrichlorosilane (FDTS) is applied on the surface of the master as a self-assembled monolayer (SAM). The FDTS is evaporated in vapor phase instead of in liquid phase to avoid insufficient wetting or non-homogeneous coating.

The ASL reduces extensively the surface energy of the silicon master, resulting in a gentle separation of the PDMS-based soft mold from silicon. The surface energy of silicon master is related to the contact angle of its liquid-gas interface, and therefore, the reduction of surface energy can be most straightforward estimated by a contact angle measurement. After ASL treatment, the contact angle of a water droplet on the silicon master reaches approx.  $115^\circ$  (Fig. 1b).

A typical PDMS product Sylgard 184 silicone is chosen as the material for making the soft mold at this structural resolution. The PDMS is replicated from the silicon master by thermal curing at  $80^\circ\text{C}$  for 2 h. The resist can be homogeneously coated on a variety of substrates with appropriate adhesion promoter.

The coated substrate is imprinted by an automated system. There has been a variety of systems on the market developed for Soft UV-NIL, like Substrate Conformal Imprint Lithography (SCIL), Air Cushion Press, SmartNIL, and way more. Taking advantage of the bowing of the soft mold, an automated imprint system employing a center-to-edge scheme at ambient atmosphere is used for imprinting throughout this work (GD-N-03, Gdnano Ltd.) (Fig. 1c) [10].

Subsequently, the residual layer from the imprint is descummed by a dry plasma process. With the resist as etch-mask, a high power and high energy plasma process is used to etch the fused silica substrate as the first study for etching at this condition of the new resist. Results and discussions will follow in the next section.

## 3. Results and discussion

In this work, the focus of investigation lies on the imprint performance and the following descumming and substrate etching. In order to access the most illustrative results, scanning electron microscopy (SEM) has been extensively employed to inspect the samples at each individual step.

The fused silica substrate is coated with hexamethyldisilazane (HMDS) as adhesion promoter, which is fully compatible with the new resist mr-NIL213FC. The HMDS is brought onto the surface of the fused silica substrate by a nitrogen ( $\text{N}_2$ ) air flow and is evaporated in an evacuated chamber at a temperature of  $95^\circ\text{C}$ .

The resist is spin-coated onto the substrate at a rotating speed of 3000 rpm for 60 s. Afterwards, the coated substrate is thermally baked at  $80^\circ\text{C}$  for 60 s. As soon as the substrate has cooled down, it is imprinted by the center-to-edge scheme at ambient atmosphere at a gentle imprint pressure of 0.5 kPa. The outcome of imprint is inspected by SEM and an exemplar imprint result is shown in tilted view and cross-sectional view respectively in Fig. 2.

The imprinted nanopillar structure owns a height of approx. 830–840 nm, which corresponds well to the master characteristics. Hence, no significant shrinkage on the lateral dimension has been observed. The nanopillar structures with an aspect ratio above two can be replicated with high fidelity into the new resist mr-NIL213FC.

The residual layer thickness has been measured accounting for approx. 80–90 nm. These values are multiply measured and roughly averaged due to the fact that the electron discharge distorts the resist polymer rather strongly after a while of beam focusing.

It has been demonstrated in previous work that the center-to-edge scheme using PDMS soft mold at ambient condition is able to support multiple consecutive imprint without mold contamination and patterning degradation [15]. With regard to the new resist, tests have been carried out in addition in a step and repeat manner, fast demonstrating that the new resist is compatible with PDMS-based soft mold for at least 191 consecutive imprints without significantly losing the pattern fidelity (Fig. 3) [11]. It shows that the resist mr-NIL213FC suits well to the PDMS soft mold causing very rare degradation.

As a subsequent process of imprint, the residual layer descumming is commonly relying on a dry plasma etching process. The plasma chemistry, i.e. mainly the etch gases, depends highly on the components of the resist. For mr-NIL213FC, which is a pure organic polymer,

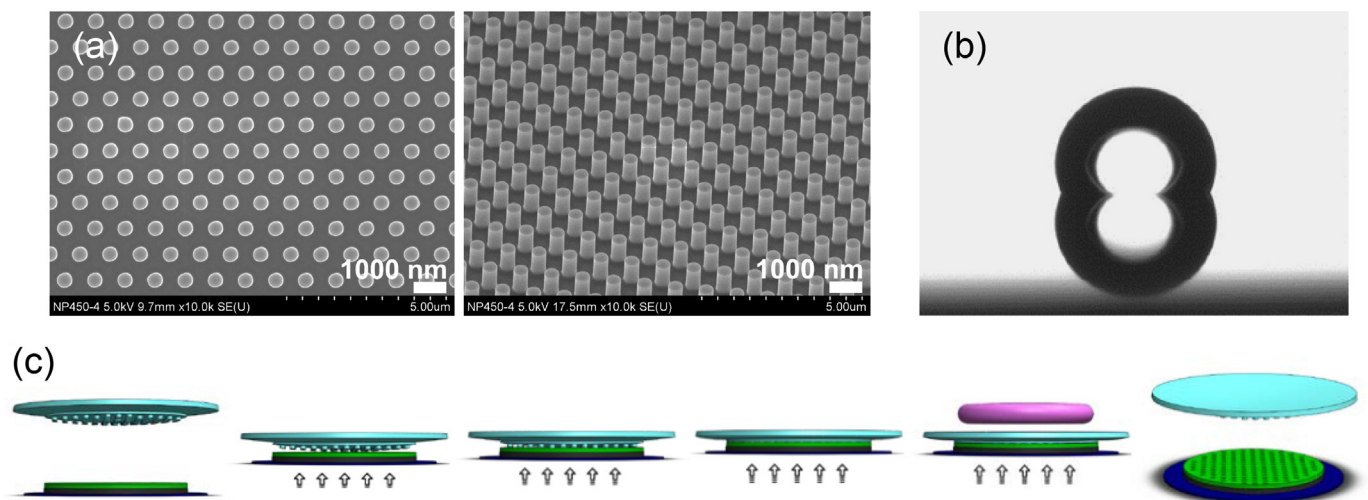


Fig. 1. NIL preparations and setup: (a) SEM images of silicon master; (b) contact angle of a water droplet of FDTD coated master; (c) schematic diagrams of imprint process.

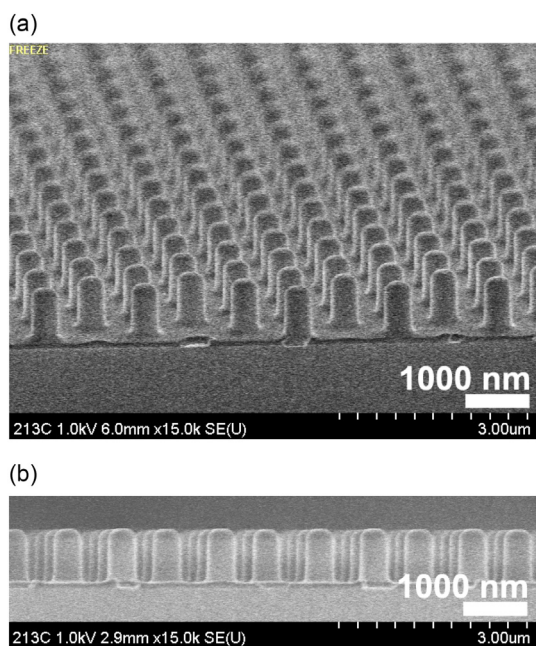


Fig. 2. SEM images of nanopillars in resist direct after imprint: (a) tilted view; (b) cross-sectional view.

can be removed simply by oxygen plasma.

According to the straightforward “one at a time” principle, a set of processing parameters have been executed, which is originated from the solid descumming recipe of preceding product mr-NIL210 series. By changing the physical power only, the descumming process undergoes the HF power from 25 W to 200 W and an optimized process has been reached at the end. Given the fact that the adhesion at the interface of resist and substrate surface changes abruptly because of the adhesion promoter, additional etching energy, therefore etching time, has to be applied to penetrate the “final nanometers” and to ensure a clean opening of substrate. It will somehow result in a slight loss of the height of the patterned nanopillars. A SEM image of a successful descumming is displayed in Fig. 4. SEM images of nanopillars in resist after residual layer descumming, and the descumming parameters are listed in Table 1. As shown in the figure, the structure height has been reduced from 850 nm down to approx. 770 nm after 40 s descumming. The etch rate that can be calculated from the shorting of patterned nanopillars

accounts for approx. 4 nm/s ((850 + 90–770) nm/40s).

A structure height of 770 nm has been taken for calculation of variations of height and depth in the subsequent etching step. The etching of fused silica is conducted with inductive coupling power (ICP) by using a fluorocarbon plasma.

Fluorocarbon plasma is widely used for etching since they chemically intend to form stable reaction products like  $\text{SiF}_4$ , CO or  $\text{CO}_2$ . The etching of fused silica is accomplished through the deposited  $\text{C}_x\text{F}_y$  polymer on the surface. Considering that the  $\text{CF}_x$  radicals do not spontaneously react with fused silica ( $\text{SiO}_2$ ), an initiation of reaction is required by ion bombardment to achieve a sufficient etch rate. In the course of the initiating reaction, the oxygen component of  $\text{SiO}_2$  reacts with the fluorocarbons to form  $\text{COF}_x$  polymers and consumes parts of the surface polymer layer. The silicon atoms chemically react with fluorine atoms to establish polymer in form of  $\text{SiF}_x$ , which can be removed easily due to its volatile nature.

The formation of surface polymer layers, on the other hand, impede the removal and surface activation, which inversely results in a decrease of etch rate. Plasma ion energy and the initiating reaction with fluorine atoms can be a great impact on this surface polymer layer. For an effective etching of  $\text{SiO}_2$  in fluorocarbon plasma, a bias voltage of higher than  $-100$  V is demanded to obtain a sufficient ratio to break the balance between the surface polymer formation and ablation [1,16]. Insufficient bias voltage may result in a drop of etch rate or in severe cases an etch stop [17–19]. However, a too high voltage can cause a decrease of the etching selectivity by a strong physical ion bombardment to the resist, and bring a high amount of heat to the underlying substrate.

As a first run with mr-NIL213FC as etch-mask with high power, a series of gas combinations using  $\text{CHF}_3$  or/and  $\text{CF}_4$  chemistry is carried out for etching into fused silica substrate. A bias voltage of  $-125$  V set consistently to provide a reasonable high physical energy for an effective  $\text{SiO}_2$  etching. The pressure is kept at 0.3 Pa and the electrode temperature is set at  $20^\circ\text{C}$ . The parameters of etch gas, flow rate, and ICP power have been changed and compared, respectively.

### 3.1. Variation of the ICP power

To begin with, the etching with the pure fluorocarbon gas  $\text{CHF}_3$  is investigated. The ICP power is stepped from 185 W, 300 W to 500 W. The increasing of ICP power enhances the plasma density in terms of its ion flux and the amount of reactive neutrals. Intense surface reactions because of the higher ion bombardment and a large amount of reactive neutrals will take place. Therefore, the etch rate can be significantly

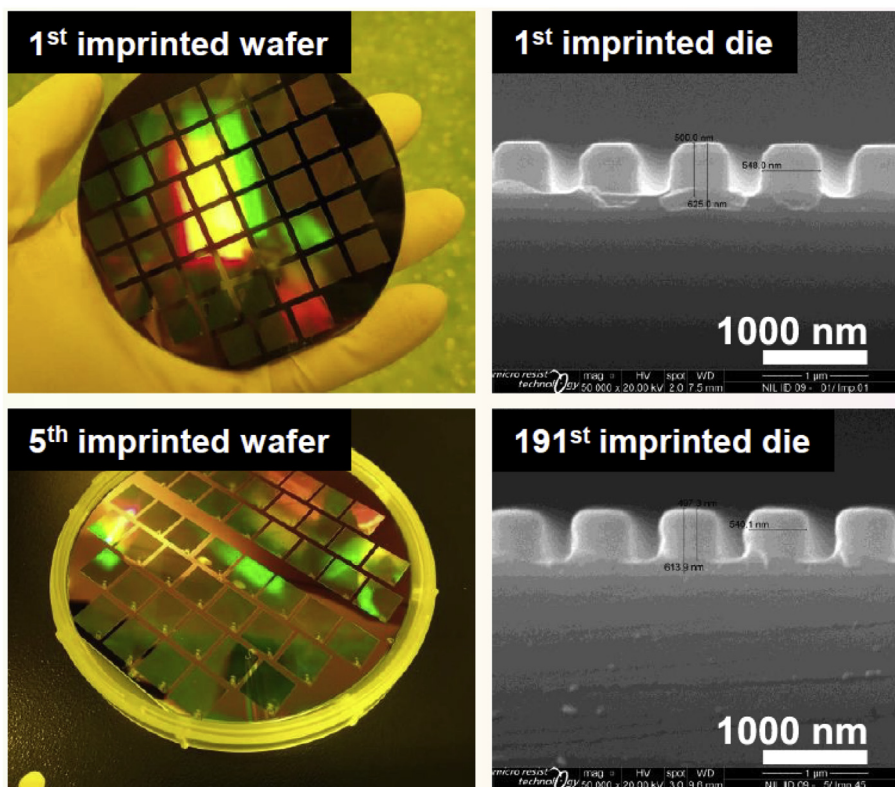


Fig. 3. Imprint by step-and-repeat on full 100 mm wafer and SEM images of the corresponding imprinted nanostructures at 1st imprint and 191st imprint.

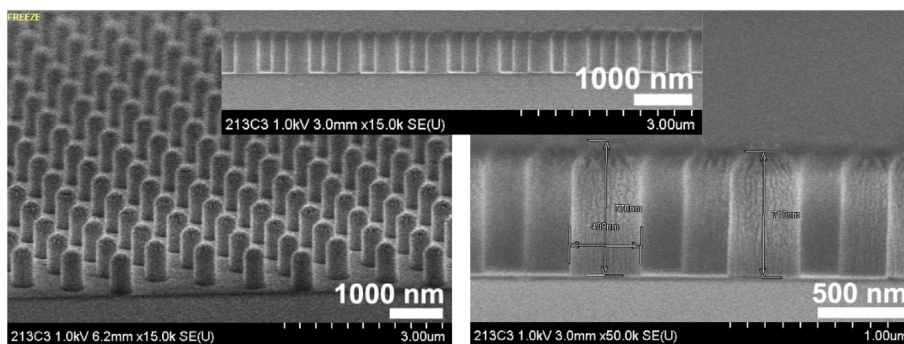


Fig. 4. SEM images of nanopillars in resist after residual layer descumming.

Table 1

Process parameters of the resist residual layer descumming.

Etch facility	Oxford Plasmalab 100
Etch gas	O <sub>2</sub>
Flow rate (sccm)	50
HF power (W)	200
Bias (V)	410
Pressure (mTorr)	100
Temperature (°C)	20
Descumming rate (nm/s)	4

Table 2

Process parameters of fused silica etching with CHF<sub>3</sub> or CF<sub>4</sub> chemistry with vary ICP powers.

Etch facility	Sentech SI 500	
Etch gas	CHF <sub>3</sub>	CF <sub>4</sub>
Flow rate (sccm)	30	30
ICP power (W)	185/300/500	185/300/500
Bias voltage (W)	-125	-125
Pressure (Pa)	0.3	0.3
Temperature (°C)	20	20

increased. Process parameters have compiled in Table 2.

The first etch results shown by SEM images have been displayed in Fig. 5. It has been observed that the corners of the nanopillars in resist mr-NIL213FC are eroded by exposing to the ion bombardment. The angle of the eroded corners associates with the maximum sputter rate. Nevertheless, the structure profile etched in fused silica is sharp with vertical sidewalls and flat smooth etch bottoms. By increasing the ICP power from 185 W to 500 W, the resist etch-mask can be slightly less

eroded, likely due to a higher polymer condensing on the surface of resist.

Etching with the same variation of ICP power as listed in Table 2 is conducted by changing the etch gas from pure CHF<sub>3</sub> to pure CF<sub>4</sub>. SEM images of the etching results are displayed in Fig. 6. It can be seen that the roughness from the physical damage on the nanopillars resist etch-mask at 300 W and 500 W is improved from that at 185 W. Moreover, in

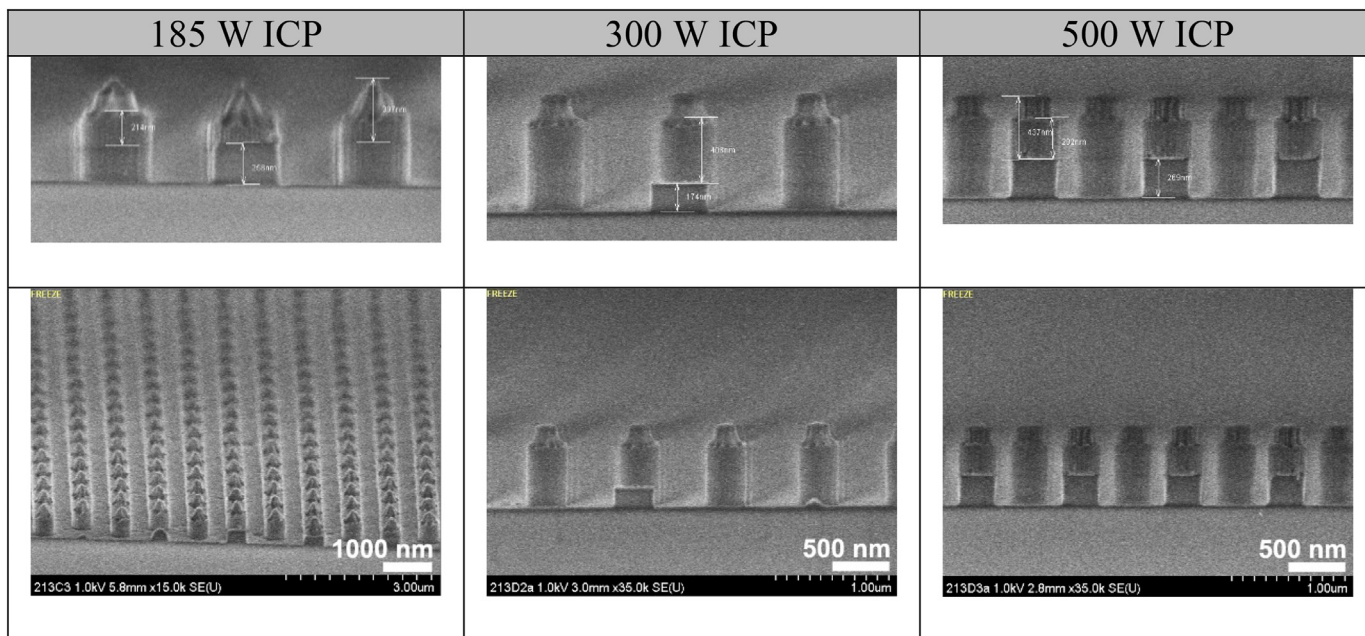


Fig. 5. SEM images of fused silica etching by CHF<sub>3</sub> with varying ICP powers, resist after the etching remains.

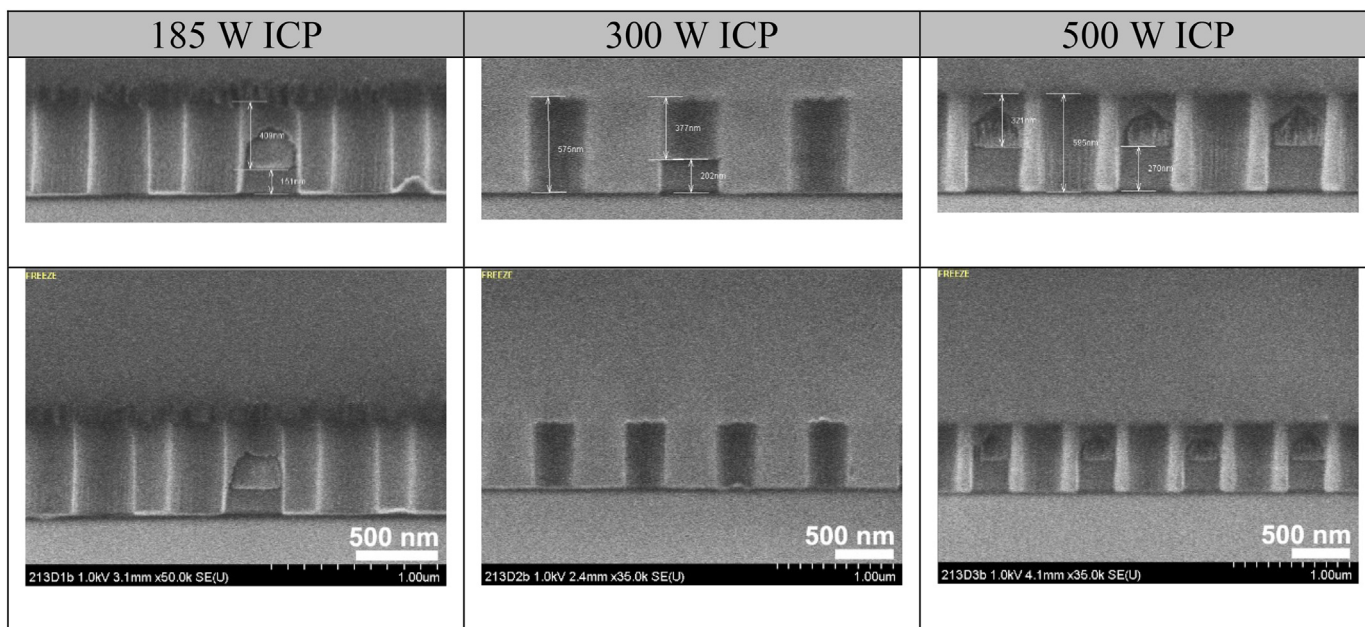


Fig. 6. SEM images of fused silica etching by CF<sub>4</sub> with varying ICP powers, resist after the etching remains.

Table 3

Process parameters of fused silica etching with a gas combination of CHF<sub>3</sub> and CF<sub>4</sub>.

Etch facility	Sentech SI 500
Etch gas	CF <sub>4</sub> and CHF <sub>3</sub>
Flow rate (sccm)	10:20/15:15/20:10
ICP power (W)	500
Bias voltage (V)	-125
Pressure (Pa)	0.3
Temperature (°C)	20

contrast to the etching using CHF<sub>3</sub> plasma, the resist etch-mask erosion is significantly reduced, leading to a higher fidelity of the resist structure in lateral dimension. Vertical sidewalls and smooth etch bottoms

have been obtained as well.

The etch rates of the fused silica substrates are enlarged with the increase of ICP power. At 500 W ICP power, the etch rate can be obtained up to 270 nm/min without strongly consuming the resist etch-mask. Based on these preliminary etching experiments, it can be roughly concluded that the higher ICP power provides an improved etch performance for both etching chemistry, which correspond well to literatures and our previous work [14,20]. The increased ICP power works sufficiently to preserve the resist etch-mask, especially when using CF<sub>4</sub> etch chemistry.

### 3.2. Variation of the CF<sub>4</sub>/CHF<sub>3</sub> mixture

The optimal etch rate and etch profile has been obtained in the first run of experiments at a ICP power of 500 W. At the next step, the ICP

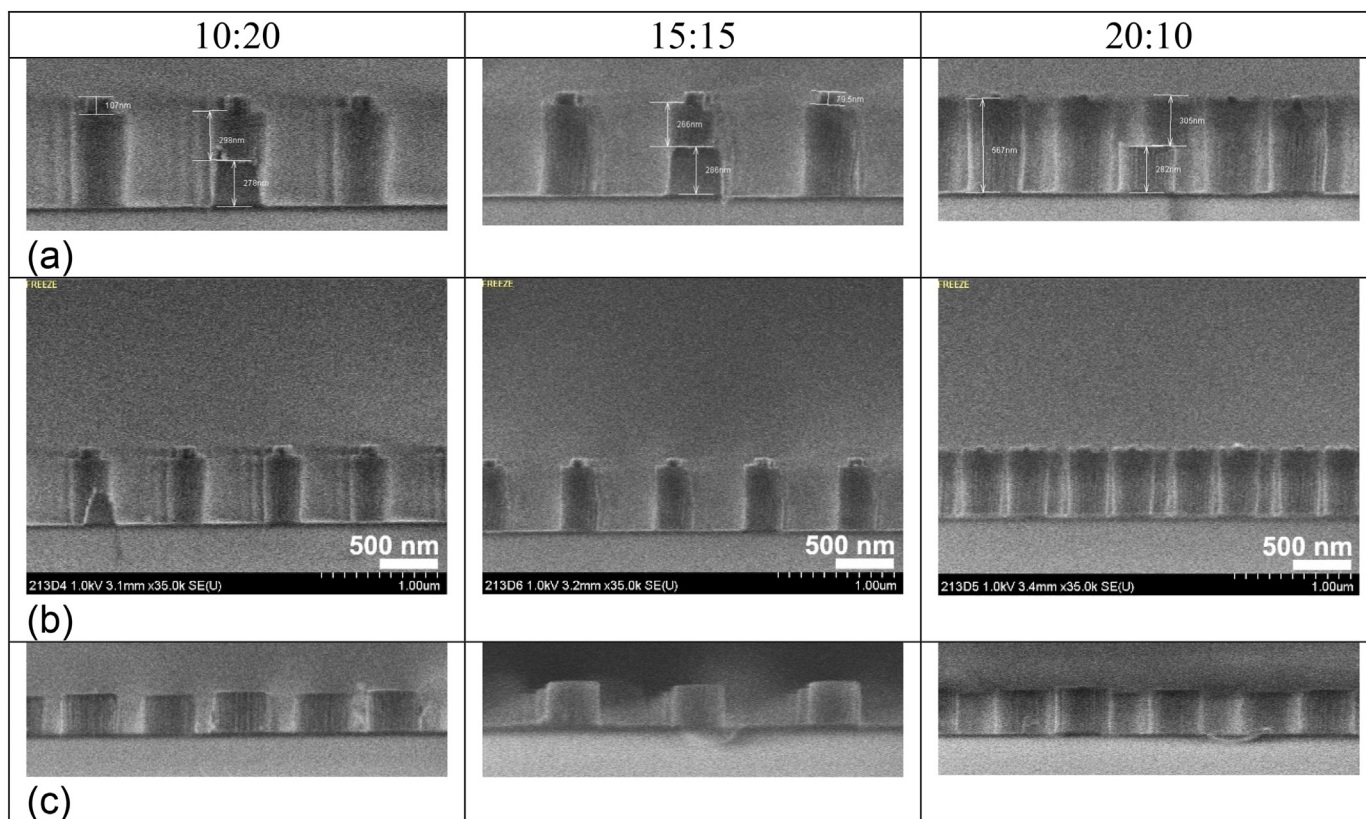


**Fig. 7.** SEM images of fused silica etching by a gas combination of  $\text{CF}_4$  and  $\text{CHF}_3$  with varying mixing ratio, resist after etching remain (a)(b), and the etched fused silica nanopillars after resist stripping (c).

**Table 4**

A summary of fused silica etching with a gas combination of  $\text{CHF}_3$  and  $\text{CF}_4$ .

Gas & Flow rate		ICP power (W)	HF power (W)	Bias (V)	Pressure (Pa)	Temperature ( $^{\circ}\text{C}$ )	Etch rate (nm/min)	Selectivity
$\text{CF}_4$	$\text{CHF}_3$							
0	30	500	200	-125	0.3	20	270	0.55
10	20						280	0.59
15	15						285	0.57
20	10						280	0.61
30	0						270	0.6

power is maintained at 500 W while a mixture of  $\text{CF}_4/\text{CHF}_3$  gases by varying mixing ratio is investigated. The mixing ratio of  $\text{CF}_4/\text{CHF}_3$  gases is set to 1:2, 1:1 and 2:1 with a fixed total flow rate of 30 sccm. The process pressure is set as 0.3 Pa, and bias voltage is kept at  $-125$  V, which are the same as the previous processes (Table 3).

SEM images of the etch results are displayed in Fig. 7. The optimal etching performance in terms of etch rate and etch selectivity lies in a gas combination that  $\text{CF}_4$  dominates (2:1). In optimal case, good etching profile for both resist etch-mask and fused silica is achieved. No significant erosion, shrinkage or corner rounding in lateral dimension is observed in the resist. The etch selectivity of mr-NIL213FC resist to the fused silica substrate reaches up to 0.61, which has been a great step-up in this context. A summary of the etching parameters as well as the calculated etch rate and selectivity is compiled in Table 4.

The etch rate and etch selectivity from the table indicate that the results lie in a very narrow range in which the difference can be neglected for a rough estimation, although the gas mixture changes rather a lot. In comparison, in microstructure etching, it has been acknowledged that an increasing amount of  $\text{CHF}_3$  leads to an enhanced binding of F-radicals and thus results in a higher polymer formation. It is also found that the ion density of  $\text{CF}_4$  plasma is generally higher compared

to that of a  $\text{CHF}_3$  plasma when using the same process parameters [20]. Besides, the etch rate of fused silica is known to be proportional to the ion density [21]. However, in the above mentioned nanostructure etching for low aspect ratio, the selectivity is obtained within a small tolerance. It can be seen that the impact of changing of gas mixture is not prominent within the very short etching duration. This correlates with the results for different electron-beam resists in previous literature [20]. Therefore, from the etch selectivity point of view, the resist performs comparably when using either fluorocarbon gases and their mixtures.

The highest etch rate possible is obtained when the  $\text{CF}_4$  and  $\text{CHF}_3$  gases take part in half of the total flow rate (15:15 sccm). Furthermore, the SEM images shown that the etch profile on the etched resist mr-NIL213FC can reach an optimal fidelity when the  $\text{CF}_4$  gas dominates. The etch profile on the fused silica, on the other hand, shows vertical sidewalls and smooth etch bottom in each case.

#### 4. Conclusion and outlook

In this work, a newly developed resist mr-NIL213FC specialized for Soft UV-NIL has been experimentally examined and verified. The resist

shows full compatibility to nanoimprint using PDMS soft molds at ambient atmosphere and is able to keep a high fidelity of nanopatterning in feature size of 400 nm and long term sustainability for up to 191 consecutive multiple imprints.

Based on the valid imprint performance, an etching using the resist mr-NIL213FC as etch-mask into fused silica substrate is carried out. The low thermal conductivity and higher binding energy of the Si-O-bonds bring extreme challenges using the polymer as etch-mask. It has been achieved that the etch selectivity of mr-NIL213FC to the fused silica can be up to, but not limited to, 0.61 for high energy plasma process, while the etch rate goes up to, but not limited to, 285 nm/min. The optimal results are obtained when CF<sub>4</sub> gas is mainly used in the etching chemistry.

It is worth noting that, although the automated NIL process has been systematically verified, the etching using the resist mr-NIL213 for fused silica has only undergone an initial experimental run. The process parameters are taken from our previous solid work, however, there is a huge space for the etching to change and to be improved. Considering that the plasma etching can strongly depend on the etch load, etch area, material, hardware parameters and such, an improvement of the etching process using the mr-NIL213FC product as well as the resist itself has been planned for the future work.

#### Declaration of Competing Interest

The authors declare that they have no known competing financial interests or personal relationships that could have appeared to influence the work reported in this paper.

#### References

- [1] Q. Zhu, L. Jin, Y. Fu, Graded index photonic crystals: a review, *Ann. Phys. (Berlin)* 527 (2015) 205–218.
- [2] S. Murthy, M. Matschuk, Q. Huang, N.K. Mandsberg, N.A. Feidenhansl, P. Johansen, L. Christensen, H. Pranov, G. Kofod, H.C. Pedersen, O. Hassager, R. Taboryski, Fabrication of nanostructures by roll-to-roll extrusion coating, *Adv. Eng. Mater.* 18 (2015) 484–489.
- [3] H. Hauser, N. Tucher, K. Tokai, P. Schneider, C. Wellens, A. Volk, S. Seitz, J. Benick, S. Barke, F. Dimroth, C. Müller, T. Glinsner, B. Bläsi, Development of nanoimprint processes for photovoltaic applications, *J. Micro/Nanolithogr. Mem. Moems* 14 (2015).
- [4] S. Zhu, H. Li, M. Yang, S.W. Pang, High sensitivity plasmonic biosensor based on nanoimprinted quasi 3D nanosquares for cell detection, *Nanotechnology* 27 (2016).
- [5] A.N. Firsov, A. Firsov, B. Loechel, A. Erko, A. Svintsov, S. Zaitsev, Fabrication of digital rainbow holograms and 3-D imaging using SEM based e-beam lithography, *Opt. Express* 23 (2014) 28756.
- [6] G.E. Moore, Cramming more components onto integrated circuits, *Electronics* 38 (1965).
- [7] D.R.S. Cumming, S.B. Furber, D.J. Paul, Beyond Moore's law, *Phil. Trans. R. Soc. A* 372 (2013).
- [8] "After Moore's law" in *Technology Quarterly, The Economist*, (2016).
- [9] M.S. Alias, M. Tangi, J.A. Holguin-Lerma, E. Stegenburgs, A.A. Alatawi, I. Ashry, R.C. Subedi, D. Priante, M.K. Shakfa, T.K. Ng, B.S. Ooi, Review of nanophotonics approaches using nanostructures and nanofabrication for III-nitrides ultraviolet-photon devices, *J. Nanophotonics* 12 (4) (2018) 043508.
- [10] S. Si, L. Dittrich, M. Hoffmann, The NanoTuFe - fabrication of large area periodic nanopatterns with tunable feature sizes at low cost, *Microelectron. Eng.* 180 (2017) 71–80.
- [11] M. Messerschmidt, M.W. Thesen, S. Si, A. Schleunitz, G. Grützner, Tailored UV-NIL resists for the fabrication of demanding photonic structures, *NIL-Industrial Day*, 2019.
- [12] M. Messerschmidt, A. Greer, F. Schlachter, J. Barnett, M.W. Thesen, N. Gadegaard, G. Grützner, A. Schleunitz, New organic photo-curable nanoimprint resist «mr-NIL210» for high volume fabrication applying soft PDMS based stamps, *J. Photopolym. Sci. Technol.* 30 (2017) 605.
- [13] M. Förthner, M. Rommel, M. Rumler, M.W. Thesen, M. Messerschmidt, mr-NIL210FC-XP – A Very Promising Resist for Employment of SCIL Technology in High Volume Industrial Applications, *SUSS report V1 07*, (2017).
- [14] C. Weigel, E. Markweg, L. Müller, M. Schulze, H. Gargouri, M. Hoffmann, A monolithic micro-optical interferometer deep etched into fused silica, *Microelectron. Eng.* 174 (2017) 40–45.
- [15] S. Si, M. Hoffmann, Consecutive imprinting performance of large area UV nanoimprint lithography using bi-layer soft stamps in ambient atmosphere, *Microelectron. Eng.* 176 (2017) 62–70.
- [16] V.M. Donnelly, A. Kornblit, Plasma etching, *J. Vac. Sci. Technol. A* 31 (2013) 50825.
- [17] G.S. Oehrlein, Surface processes in low pressure plasmas, *Surf. Sci.* (1997) 222–230.
- [18] T.E.F.M. Standaert, C. Hedlund, E.A. Joseph, G.S. Oehrlein, T.J. Dalton, Role of fluorocarbon film formation in the etching of silicon, silicon dioxide, silicon nitride, and amorphous hydrogenated silicon carbide, *J. Vac. Sci. Technol. A* (2004) 53–60.
- [19] M. Schaeepkens, G.S. Oehrlein, A review of SiO<sub>2</sub> etching studies in inductively coupled fluorocarbon plasmas, *J. Electrochem. Soc.* C211 (2001).
- [20] C. Weigel, M. Schulze, H. Gargouri, M. Hoffmann, Deep etching of Zerodur glass ceramics in a fluorine-based plasma, *Microelectron. Eng.* 185–186 (2018) 1–8.
- [21] Ch. Steinbrüchel, Langmuir Probe Measurements on CHF<sub>3</sub> and CF<sub>4</sub> Plasmas: The Role of Ions in the Reactive Sputter Etching of SiO<sub>2</sub> and Si, (1983).